H1-prelim-02-031
April 2002

FORWARD π^0 MESON PRODUCTION AT HERA

H1 Collaboration

Abstract

The dynamics of QCD evolution at low values of Bjorken-x is studied via the measurement of hard π^0 probes which are produced near to the fragmenting proton direction (the forward region) in deeply inelastic positron proton scattering at the H1 experiment. Measurements of the forward π^0 cross-section and the accompanying transverse energy flow around the π^0 are presented and used to discriminate between models which implement different schemes for QCD evolution.

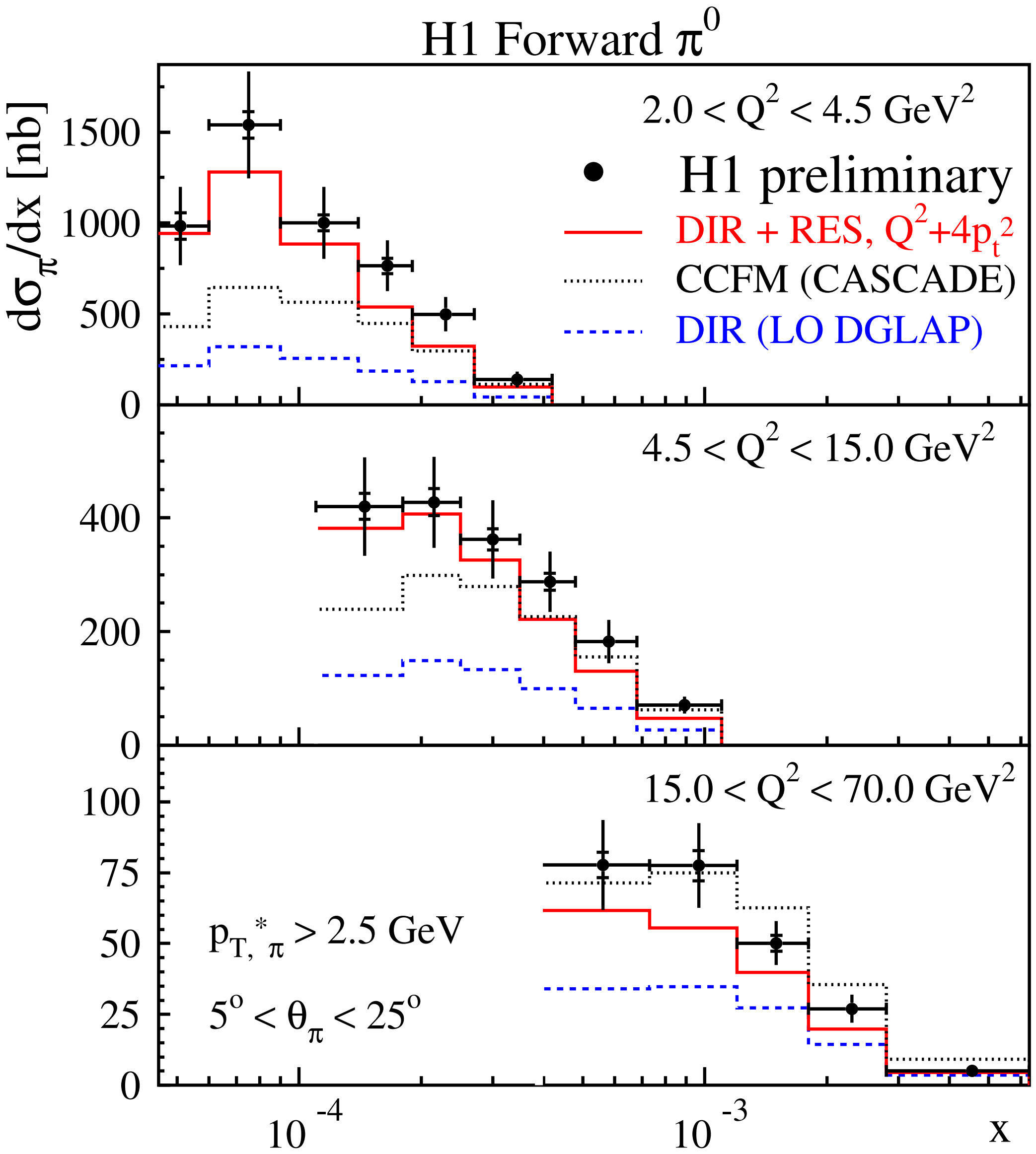

Figure 1: Inclusive π^0-meson production cross-sections as a function of x for $p^*_{T,\pi} >$ 2.5 GeV in three regions of Q^2. The phase space is defined by $0.1 < y < 0.6$, $x_\pi = E_\pi/E_{proton} > 0.01$, θ_π and Q^2 ranges given in the figure. The inner bars are statistical, the outer error bars give the statistical and systematical error added quadratically. The QCD models based on LO DGLAP parton showers with (DIR+RES) and without (DIR) resolved photon processes and on the implementation of the CCFM equation are compared to the data.

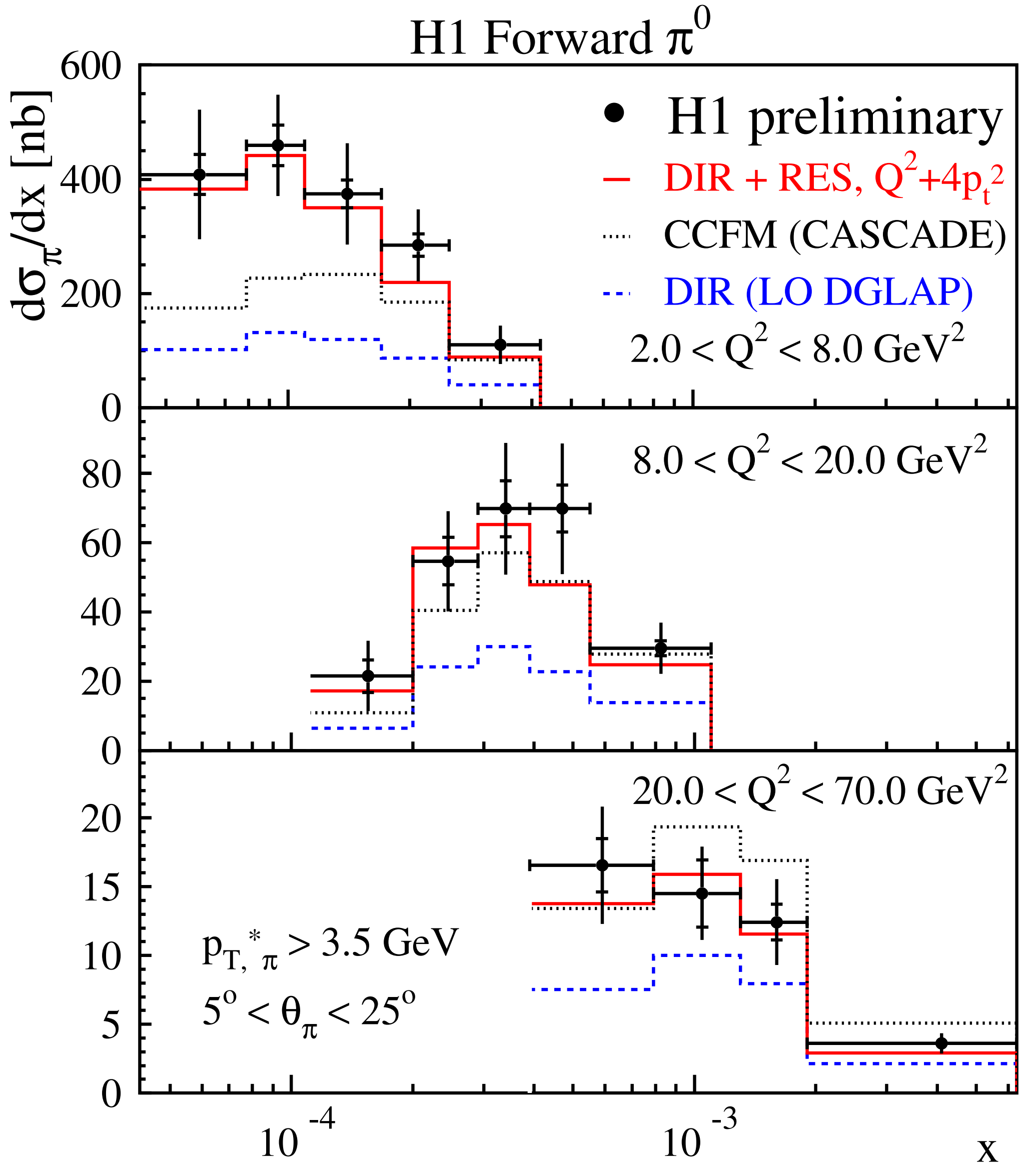

Figure 2: Inclusive π^0-meson production cross-sections as a function of x for $p^*_{T,\pi} > 3.5$ GeV in three regions of Q^2. The phase space is defined by $0.1 < y < 0.6$, $x_\pi = E_\pi/E_{proton} > 0.01$, θ_π and Q^2 ranges given in the figure. The inner bars are statistical, the outer error bars give the statistical and systematical error added quadratically. The QCD models based on LO DGLAP parton showers with (DIR+RES) and without (DIR) resolved photon processes and on the implementation of the CCFM equation are compared to the data.

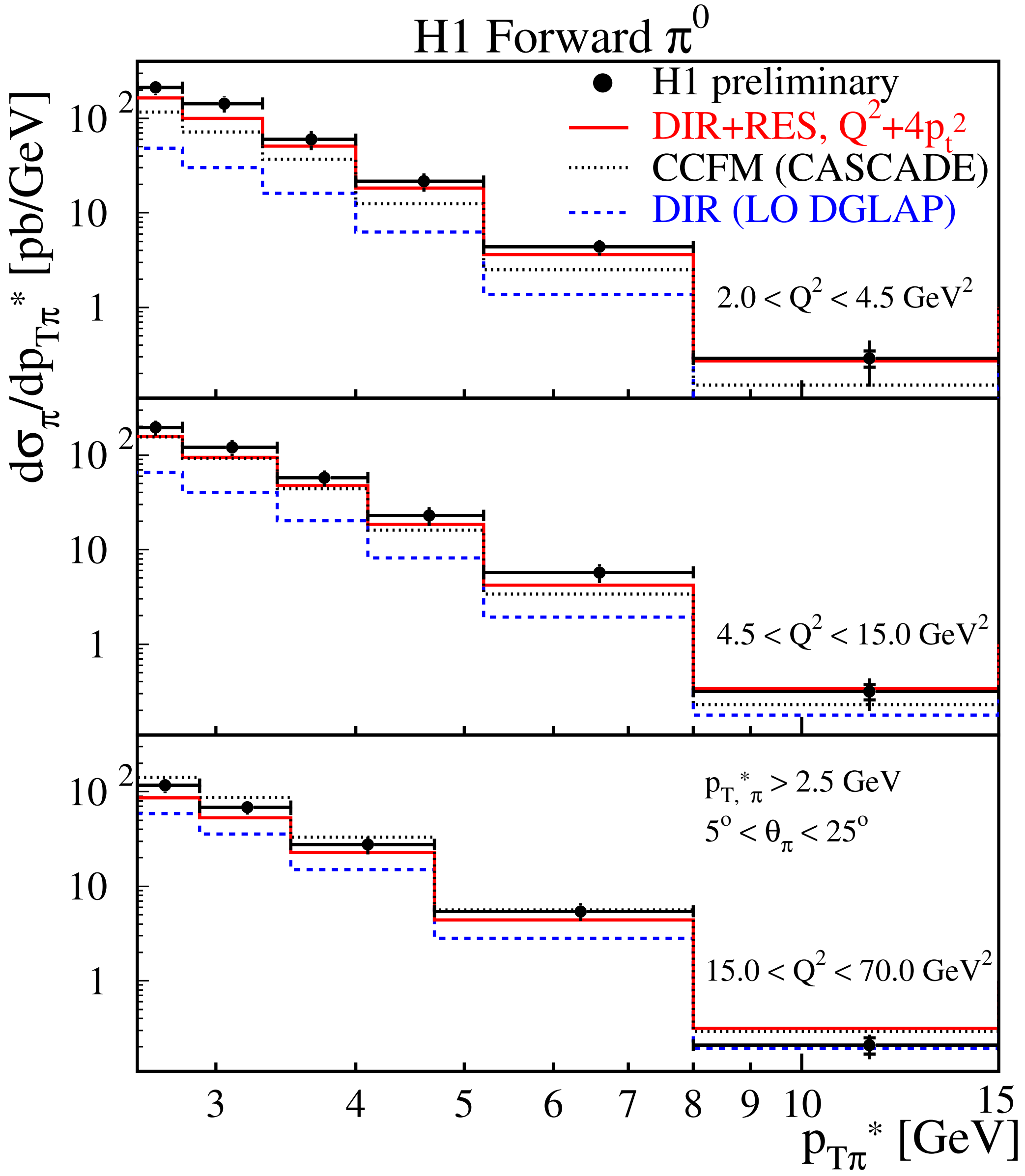

Figure 3: Inclusive π^0-meson production cross-sections as a function of $p^*_{T,\pi}$ for $p^*_{T,\pi} > 2.5$ GeV in three regions of Q^2. The phase space is defined by $0.1 < y < 0.6$, $x_\pi = E_\pi/E_{proton} > 0.01$, θ_π and Q^2 ranges given in the figure. The inner bars are statistical, the outer error bars give the statistical and systematical error added quadratically. The QCD models based on LO DGLAP parton showers with (DIR+RES) and without (DIR) resolved photon processes and on the implementation of the CCFM equation are compared to the data.

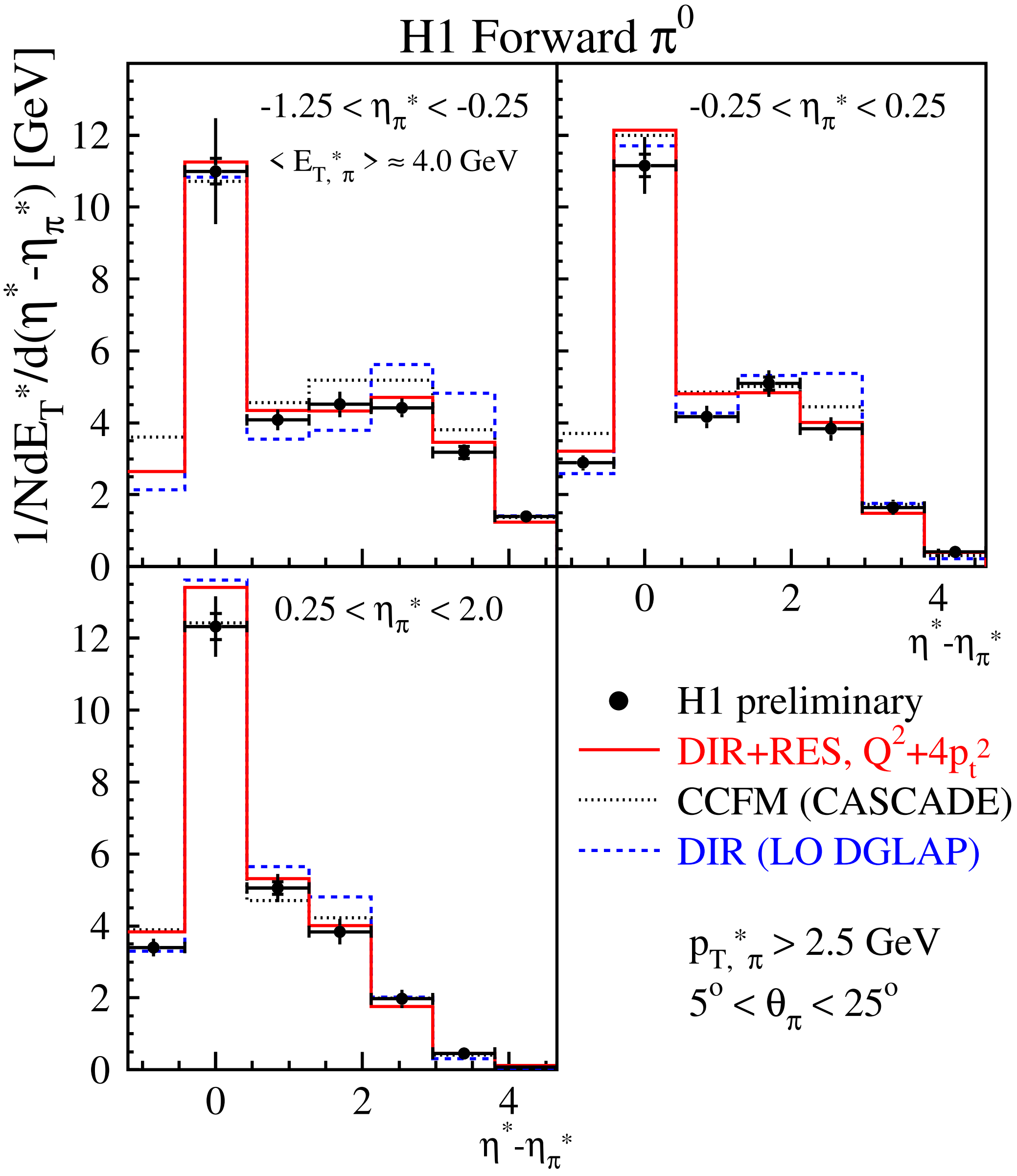

Figure 4: Transverse energy flow around the forward π^0 for different ranges of η^*_π in the hadronic CMS as a function of the distance from the π^0 direction. The incoming photon direction defines the $+z^*$ direction. The contribution from the forward π^0 is included in the distributions and marked on the plots. The phase space is defined by $2.0 < Q^2 < 70.0\ GeV^2$, $0.1 < y < 0.6$, $x_\pi = E_\pi/E_{proton} > 0.01$, θ_π and $p^*_{T,\pi}$ ranges given in the figure. The inner bars are statistical, the outer error bars give the statistical and systematical error added quadratically. The QCD models based on LO DGLAP parton showers with (DIR+RES) and without (DIR) resolved photon processes and on the implementation of the CCFM equation are compared to the data.

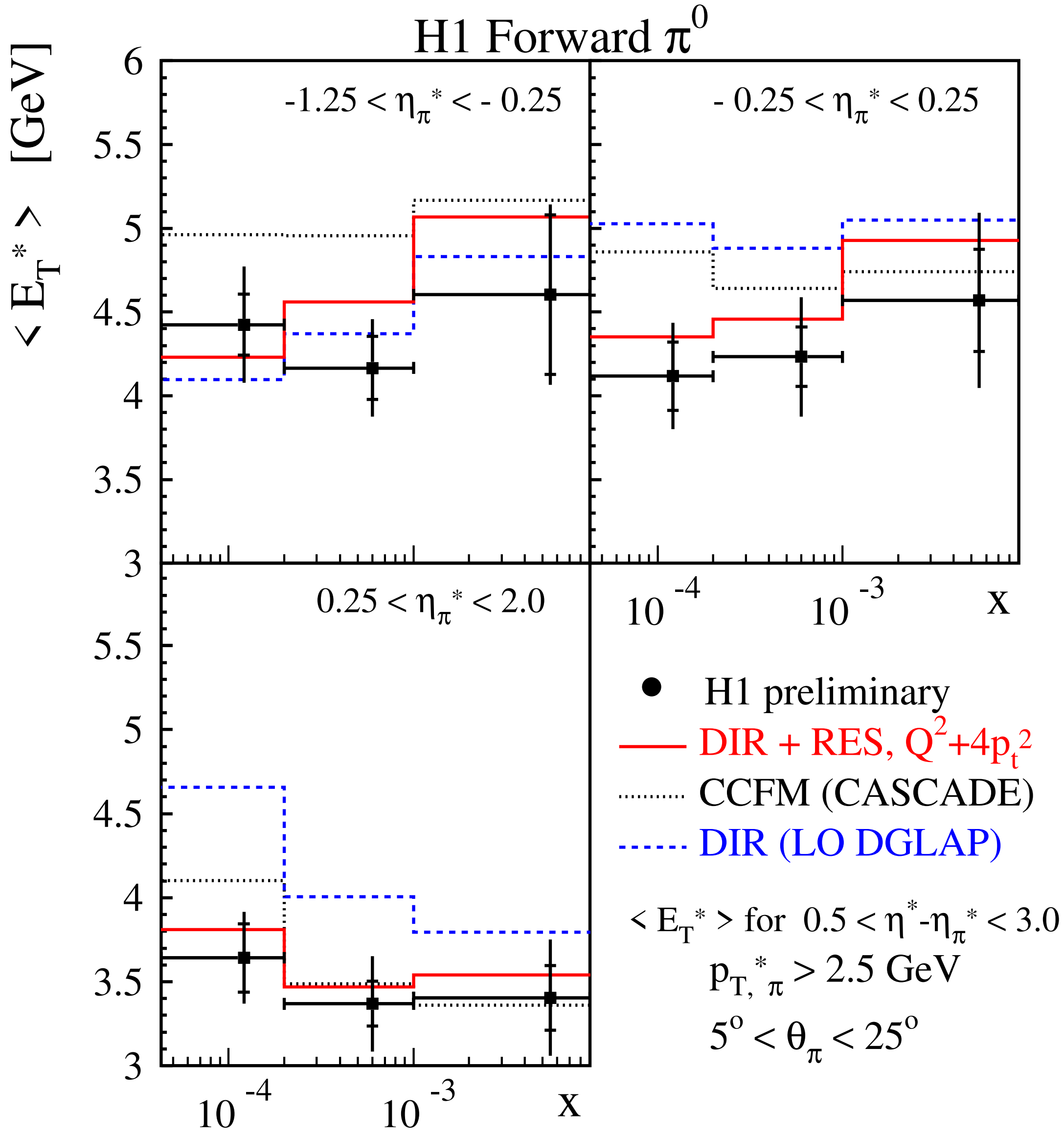

Figure 5: Mean transverse energy in the region $0.5 < \eta^* - \eta^*_\pi < 3.0$ for different ranges of η^*_π in the hadronic CMS as a function of Bjorken x. The phase space is defined by $2.0 < Q^2 < 70.0\ GeV^2$, $0.1 < y < 0.6$, $x_\pi = E_\pi/E_{proton} > 0.01$, θ_π and $p^*_{T,\pi}$ ranges given in the figure. The inner bars are statistical, the outer error bars give the statistical and systematical error added quadratically. The QCD models based on LO DGLAP parton showers with (DIR+RES) and without (DIR) resolved photon processes and on the implementation of the CCFM equation are compared to the data.